units in sarcosine oxidase is involved in the binding of folates and sarcosine.

ACKNOWLEDGMENTS

We thank Juanita Yee-Foon Peck for excellent technical assistance.

REFERENCES

Ackers, G. K. (1973) *Methods Enzymol. 27*, 441–455.
Chen, M. S., & Schirch, L. (1972) *J. Biol. Chem. 248*, 3631–3635, 7979–7984.
Cook, R. J., Misono, K. S., & Wagner, C. (1984) *J. Biol. Chem. 259*, 12475–12480.
Foo, S. K., Cichowicz, D. S., & Shane, B. (1980) *Anal. Biochem. 107*, 109–115.
Hayashi, S., Nakamura, S., & Suzuki, M. (1980) *Biochem. Biophys. Res. Commun. 96*, 924–930.
Hayashi, S., Suzuki, M., & Nakamura, S. (1982) *Biochem. Int. 4*, 617–620.
Hayashi, S., Suzuki, M., & Nakamura, S. (1983) *J. Biochem. (Tokyo) 94*, 551–558.
Hummel, J. P., & Dreyer, W. J. (1962) *Biochim. Biophys. Acta 63*, 530–532.
Jorns, M. S. (1985) *Biochemistry 24*, 3189–3194.
Jorns, M. S., & Hersh, L. B. (1975) *J. Biol. Chem. 250*, 3620–3628.
Kallen, R. G. (1971) *Methods Enzymol. 18*, 705–716.
Kvalnes-Krick, K., & Jorns, M. S. (1986) *Biochemistry 25*, 6061–6069.
Matthews, R. G., & Baugh, C. M. (1980) *Biochemistry 19*, 2040–2045.
Patek, D. R., & Frisell, W. R. (1972) *Arch. Biochem. Biophys. 150*, 347–354.
Porter, D. H., Cook, R. J., & Wagner, C. (1985) *Arch. Biochem. Biophys. 243*, 396–407.
Ramasastri, B. V., & Blakley, R. L. (1964) *J. Biol. Chem. 239*, 106–111.
Sato, M., Ohnishi, N., & Yagi, K. (1981) *Biochem. Int. 3*, 89–92.
Scatchard, G. (1949) *Ann. N.Y. Acad. Sci. 51*, 660–672.
Scrimgeour, K. G. (1980) *Methods Enzymol. 66*, 517–523.
Steenkamp, D. J., & Husain, M. (1982) *Biochem. J. 203*, 707–715.
Suzuki, M. (1981) *J. Biochem. (Tokyo) 89*, 599–607.
Wittwer, A. J., & Wagner, C. (1981) *J. Biol. Chem. 256*, 4102–4108.

Infrared Studies of Fully Hydrated Unsaturated Phosphatidylserine Bilayers. Effect of Li^+ and Ca^{2+} †

H. L. Casal,* A. Martin, and H. H. Mantsch
Division of Chemistry, National Research Council of Canada, Ottawa, Canada K1A 0R6
F. Paltauf
Institut für Biochemie und Lebensmittelchemie, Technische Universität Graz, A-8010 Graz, Austria
H. Hauser
Laboratorium für Biochemie, ETH-Zentrum, CH-8092 Zürich, Switzerland
Received March 18, 1987; Revised Manuscript Received June 24, 1987

ABSTRACT: Infrared spectroscopy has been used to characterize the thermal-phase behavior of fully hydrated 1-palmitoyl-2-oleoyl-*sn*-glycero-3-phospho-L-serine (POPS) and 1,2-dioleoyl-*sn*-glycero-3-phospho-L-serine (DOPS) as well as their interaction with Li^+ and Ca^{2+}. The order–disorder transition of POPS–NH_4^+ is at 17 °C; in the presence of Li^+ a POPS–Li^+ complex is formed, and the transition temperature of this complex is 40 °C. DOPS–NH_4^+ has an order–disorder transition at −11 °C, and unlike POPS the addition of Li^+ has no effect on the thermal behavior of DOPS–NH_4^+. This indicates that the binding of Li^+ to DOPS is negligible or very weak. Li^+ binds to the phosphate and carboxylate groups of POPS, and as a result these groups lose their water of hydration. Li^+ binding induces a conformational change, probably in the glycerol backbone of POPS; however, the conformation of the two P–O ester bonds remains gauche–gauche as in POPS–NH_4^+. Both POPS and DOPS form crystalline complexes with Ca^{2+}. As a result of Ca^{2+} binding to the phosphate, this group loses its water of hydration and there is a conformational change in the P–O ester bonds from gauche–gauche to antiplanar–antiplanar. In contrast to the POPS–Li^+ complex, the carboxylate group remains hydrated in the Ca^{2+} complexes. Furthermore, in these PS–Ca^{2+} complexes a new hydrogen bond is formed between one of the ester C=O groups and probably water. Such a situation is not found in the NH_4^+ and Li^+ salts of phosphatidylserine.

The study of the interaction of metal ions with membrane lipids continues to be a subject of considerable interest. Such studies are generally aimed at advancing our understanding of the basic properties of lipid assemblies and, in the case of Li^+ and Ca^{2+} binding to PS,[1] possible physiological implications are of interest (Schou, 1976; Papahadjopoulos, 1978; Wilschut et al., 1981; Ohki, 1982). The macroscopic properties of both Li^+ and Ca^{2+} complexes with different saturated phosphatidylserines (PS) have been investigated by physical techniques such as calorimetry and X-ray diffraction (Jacobson

† Issued as NRCC Publication No. 28178. This work was supported by the Swiss National Science Foundation (Grant 3,579-0.84).

[1] Abbreviations: PS, phosphatidylserine; DMPS, 1,2-dimyristoyl-*sn*-glycero-3-phospho-L-serine; POPS, 1-palmitoyl-2-oleoyl-*sn*-glycero-3-phospho-L-serine; DOPS, 1,2-dioleoyl-*sn*-glycero-3-phospho-L-serine; GPS, *sn*-glycero-3-phospho-L-serine; Tes, 2-[[2-hydroxy-1,1-bis(hydroxymethyl)ethyl]amino]ethanesulfonic acid; EDTA, ethylenediaminetetraacetic acid.

0006-2960/87/0426-7395$01.50/0 Published 1987 by the American Chemical Society

& Papahadjopoulos, 1975; Hauser & Shipley, 1984, 1985). Several spectroscopic methods have also been applied to studies of PS–Ca^{2+} complexes (Kurland et al., 1979; Holwerda et al., 1981; Dluhy et al., 1983). In general, it is well established that both Li^+ and Ca^{2+} induce an isothermal crystallization of the PS fatty acyl chains in saturated PS and that the head group becomes dehydrated in the presence of these metal ions. We reported infrared and ^{31}P NMR studies of dried ("anhydrous") samples of PS–Li^+ and PS–Ca^{2+} complexes (Casal et al., 1987a). The differences in the mode of Li^+ and Ca^{2+} binding to fully hydrated 1,2-dimyristoyl-*sn*-glycero-3-phospho-L-serine (DMPS) were the subject of a recent infrared study (Casal et al., 1987b).

In this paper we present a detailed investigation of the effect of metal ions on fully hydrated unsaturated phosphatidylserines by infrared spectroscopy. For this investigation we have used 1-palmitoyl-2-oleoyl-*sn*-glycero-3-phospho-L-serine (POPS) and 1,2-dioleoyl-*sn*-glycero-3-phospho-L-serine (DOPS). These two phospholipids contain one and two oleoyl chains, respectively, and therefore differ in unsaturation and hence in cross-sectional area and surface charge density. The present results taken together with those obtained previously on the fully saturated DMPS (Casal et al., 1987b) give a clear picture regarding the effect of the lipid cross-sectional area on the strength of metal–ion binding. The differences in the mode of Li^+ and Ca^{2+} binding as reported for DMPS were also found for the unsaturated phospholipids POPS and DOPS.

Materials and Methods

1-Palmitoyl-2-oleoyl-*sn*-glycero-3-phospho-L-serine (POPS) and 1,2-dioleoyl-*sn*-glycero-3-phospho-L-serine (DOPS) were synthesized and purified as described previously (Hermetter et al., 1982; Casal et al., 1987a). In this study the monoammonium salts of both POPS and DOPS were used. Precipitates of POPS and DOPS with Li^+ and Ca^{2+} were prepared by adding LiCl and $CaCl_2$ in buffer (100 mM NaCl, 2 mM Tes, 2 mM His, 0.1 mM EDTA, pH 7, prepared in D_2O) to ready-made unsonicated dispersions of POPS and DOPS in the same buffer. In general, the samples were 0.15 M in lipid and contained different amounts of Li^+ or Ca^{2+} to yield samples of various compositions. The precipitates thus formed are referred to as aqueous precipitates. For infrared measurement, the aqueous precipitates were deposited on CaF_2 or BaF_2 windows and assembled into cells of 12-μm path length.

Infrared spectra at 2-cm^{-1} resolution were collected with a Digilab FTS-15 Fourier transform spectrometer; for each spectrum 200 interferograms were averaged. Procedures for data collection and analysis have been described previously (Casal & Mantsch, 1984; Mantsch et al., 1986). In particular, in order to separate broad band contours into their constituent bands, Fourier deconvolution techniques (Kauppinen et al., 1981) were applied. The broad bands in the spectral region 1800–1550 cm^{-1} were deconvolved with Lorentzian lines of 15 cm^{-1} full width at half-height and a resolution enhancement factor of 2.

Results and Discussion

The Li^+ and Ca^{2+} complexes of POPS and DOPS were investigated by analyzing their infrared spectra in comparison with those of the corresponding NH_4^+ salts. Since complexation with Li^+ and Ca^{2+} involves changes in the thermotropic phase behavior of these lipids, we give in Table I the relevant thermal information as measured by DSC (Demel et al., 1987). We note that in the case of samples containing Ca^{2+} or Li^+ a large excess (0.5 M) of metal ions was used in DSC measurements but not in infrared experiments; this difference in ion concentration may account for differences in the transition temperatures determined by DSC and infrared (vide infra).

Table I: Transition Temperatures T_m of Natural and Synthetic Diacylphosphatidylserines in the Absence and Presence of Cations[a]

phosphatidylserine	T_m (°C)	exptl conditions[b]
DMPS–NH_4^+	40 ± 1	5 mM phosphate buffer, pH 6.8
DMPS–Li^+	90 ± 1	as above + excess Li^+
DMPS–Ca^{2+}	155 ± 3	as above + excess Ca^{2+}
ox brain PS–Na^+	14.5 ± 0.5	5 mM phosphate buffer, pH 7, 5 mM EDTA
ox brain PS–Li^+	52 ± 2	as above + excess Li^+
ox brain PS–Ca^{2+}	120 ± 3	as above + excess Ca^{2+}
POPS–NH_4^+	13 ± 1	5 mM Tris buffer, pH 7
POPS–Na^+	13 ± 1	as above
POPS–Li^+	50 ± 1	as above + excess Li^+
POPS–Ca^{2+}	120 ± 3	as above + excess Ca^{2+}
DOPS–Na^+	−11 ± 1	5 mM phosphate buffer, pH 7, 5 mM EDTA
DOPS–Li^+	*c*	as above + excess Li^+
DOPS–Ca^{2+}	120 ± 3	as above + excess Ca^{2+}

[a] Data from Demel et al. (1987). [b] In order to obtain an excess cation (Li^+ and Ca^{2+}) concentration, the same buffers were used but containing 0.5 M LiCl or $CaCl_2$. The cationic excess varies from 5 to 20 times depending on the concentration of lipid used. [c] No transition observed between the ice-melting temperature and 150 °C.

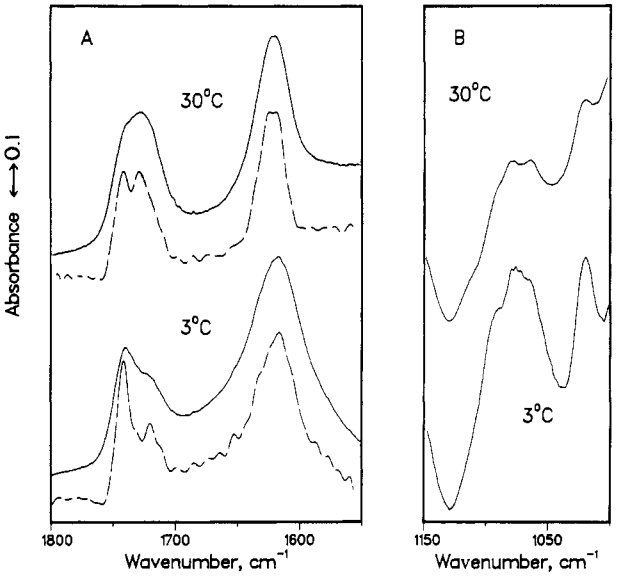

FIGURE 1: Infrared spectra in the 1800–1550- (A) and 1150–1000-cm^{-1} (B) regions of fully hydrated POPS–NH_4^+ at 3 and 30 °C. The dotted lines in part A are the result of deconvolution (see Materials and Methods).

(A) Infrared Spectra of POPS–NH_4^+ and DOPS–NH_4^+. To serve as reference for comparison with the spectra of the Li^+ and Ca^{2+} complexes of POPS and DOPS, we present here a brief description of the infrared spectra of POPS–NH_4^+ and DOPS–NH_4^+. Figure 1 shows the infrared spectra of hydrated POPS–NH_4^+ at 3 and 30 °C in the 1800–1550-cm^{-1} region (part A) and in the 1150–1000-cm^{-1} region (part B). As is evident from Table I, the two spectra recorded at 3 and 30 °C correspond to the gel and liquid-crystalline phases of POPS–NH_4^+, respectively. In the gel-phase spectrum (Figure 1A), the ester carbonyl stretching mode, $\nu_{C=O}$, gives rise to two bands of different intensities at 1740 and 1720 cm^{-1}; in the liquid-crystalline phase these two bands are at 1740 and 1728 cm^{-1} but are of similar intensities. Such spectral behavior is typical of diacyl lipids, and the origin of these two bands has been described (Mushayakarara & Levin, 1982; Levin, 1984).

The band due to the antisymmetric stretching mode of the carboxylate group, $\nu_{as}(CO_2)$, is at 1620 cm^{-1} in the gel phase

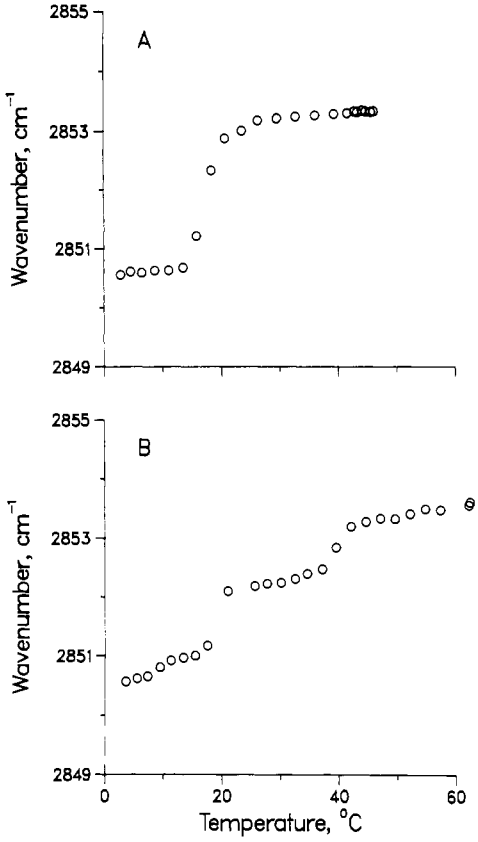

FIGURE 2: Temperature dependence of the wavenumber of the $\nu_s(CH_2)$ band in the infrared spectra of samples containing (A) 0.15 M POPS–NH_4^+ and (B) 0.15 M LiCl and 0.15 M POPS–NH_4^+ (POPS/Li^+ molar ratio = 1.0). In both cases, the samples were dispersed in D_2O buffer, pH 7.

and at 1625 cm^{-1} in the liquid-crystalline phase. The same behavior has been found in the spectra of DMPS–NH_4^+. These values of the $\nu_{as}(CO_2)$ mode are indicative of the carboxylate group being hydrated in both the gel and the liquid-crystalline phases of POPS–NH_4^+.

The spectra of Figure 1B show the bands due to the PO_2^- symmetric stretching, $\nu_s(PO_2)$, of POPS–NH_4^+. The pattern of these bands is the same as in the case of DMPS–NH_4^+ (Casal et al., 1987b) and other diacyl lipids (Casal & Mantsch, 1984), and it has been associated with the phosphate group being in the gauche–gauche conformation (Casal et al., 1987a). These bands are not particularly sensitive to the gel to liquid-crystal transition, and therefore the spectra at 3 and 30 °C are not very different.

The spectra of hydrated DOPS–NH_4^+ are practically the same as those of POPS–NH_4^+ shown in Figure 1. Thus, they can be used as reference for comparison with the spectra of DOPS–Li^+ and DOPS–Ca^{2+}.

(B) Infrared Spectra of POPS–Li^+ and DOPS–Li^+. The thermotropic phase behavior of membrane lipids can be conveniently monitored through the temperature dependence of the wavenumber of the CH_2 symmetric stretching mode, $\nu_s(CH_2)$, of the CH_2 groups in the fatty acyl chains of the phospholipid. Figure 2 shows the temperature dependence of the $\nu_s(CH_2)$ wavenumber in the spectra of hydrated POPS–NH_4^+ (Figure 2A) and the aqueous precipitates of POPS–Li^+ (Figure 2B). The particular sample from which the data in Figure 2B were obtained contained equimolar amounts of Li^+ and POPS (molar ratio POPS/Li^+ = 1.0).

The data of Figure 2A indicate that at 17 °C there is an order–disorder transition of POPS–NH_4^+ reflected in a wavenumber increase from 2850.8 to 2853.0 cm^{-1}. The value of 17 °C for the transition temperature of POPS–NH_4^+ is in agreement with the transition temperature of POPS–NH_4^+ measured by DSC (Table I). This transition represents the chain conformational melting whereby disorder is introduced in the phospholipid fatty acyl chains. The values of the wavenumbers observed below and above the transition temperature T_1 are typical of gel-phase and liquid-crystalline-phase lipids, respectively (Casal & Mantsch, 1984).

The data obtained from spectra of POPS–Li^+ (Figure 2B) indicate that in the presence of Li^+ there are two order–disorder transitions manifested in the two increases in $\nu_s(CH_2)$ wavenumber. These transitions are at 18 and 40 °C. The transition at 18 °C can be identified with T_1, the gel to liquid-crystalline transition temperature of uncomplexed POPS–NH_4^+. The transition at 40 °C (T_2) represents the conformational melting of the POPS–Li^+ complex.

The temperature dependence of the $\nu_s(CH_2)$ wavenumber indicates that POPS binds to Li^+, forming a complex with a gel to liquid-crystalline transition at 40 °C, i.e., some 23 °C higher than the transition temperature of POPS–NH_4^+. DSC measurements showed a transition at 50 °C for POPS in the presence of excess Li^+ (Table I). Thus, the infrared data on POPS are in accord with the DSC results, taking into account the different experimental conditions.

In principle, the thermal response of POPS–Li^+ indicates that in the Li^+ complex the fatty acyl chains of POPS are more ordered than in POPS–NH_4^+ since the conformational melting occurs at higher temperature. The temperature difference between T_1 (transition temperature of POPS–NH_4^+) and T_2 (transition temperature of POPS–Li^+) is 22 °C when both occur in the same sample (Figure 2B). In the case of DMPS–Li^+ (Casal et al., 1987b) the difference between T_1 and T_2 in samples of comparable molar ratios is more than 45 °C, and T_1 is only seen as a very minor increase in wavenumber. In the POPS–Li^+ sample, there is apparently a high enough concentration of uncomplexed POPS–NH_4^+ to give rise to a considerable increase in wavenumber at T_1 (the increase at T_1 is actually larger than that at T_2). These differences in the thermal behavior of POPS and DMPS in the presence of Li^+ suggest that DMPS has a higher affinity for Li^+ than POPS. This is probably a consequence of the smaller cross-sectional area and increased surface charge density of DMPS. Differences in Li^+ binding to DMPS and POPS were also found in our ^{31}P NMR study (Casal et al., 1987a) as well as in a monolayer study (Demel et al., 1987).

The temperature dependence of the $\nu_s(CH_2)$ wavenumber in the spectra of DOPS–NH_4^+ and DOPS–Li^+ (DOPS/Li^+ molar ratio = 1.0) is shown in parts A and B of Figure 3, respectively. These data indicate that there is an order–disorder transition at about −10 °C in DOPS–NH_4^+ (Figure 3A) followed by a further increase in wavenumber at 4 °C induced by ice melting (in this case D_2O). These results are in excellent agreement with the DSC results given in Table I. The temperature dependence of the $\nu_s(CH_2)$ wavenumber from the spectra of DOPS–Li^+ (Figure 3B) is practically the same as that of DOPS–NH_4^+. There is no second transition at higher temperatures at a molar ratio DOPS/Li^+ of 1.0. At this mole ratio or even with an excess of Li^+, DSC measurements show that there is no order–disorder transition in the temperature range 0–120 °C. The close similarity in the temperature dependence of $\nu_s(CH_2)$ of DOPS–NH_4^+ and DOPS–Li^+ indicates that even if a DOPS–Li^+ complex is formed, its thermal properties are indistinguishable from those of DOPS–NH_4^+. This is in agreement with ^{31}P NMR (Casal et al., 1987a) and DSC results (Demel et al., 1987).

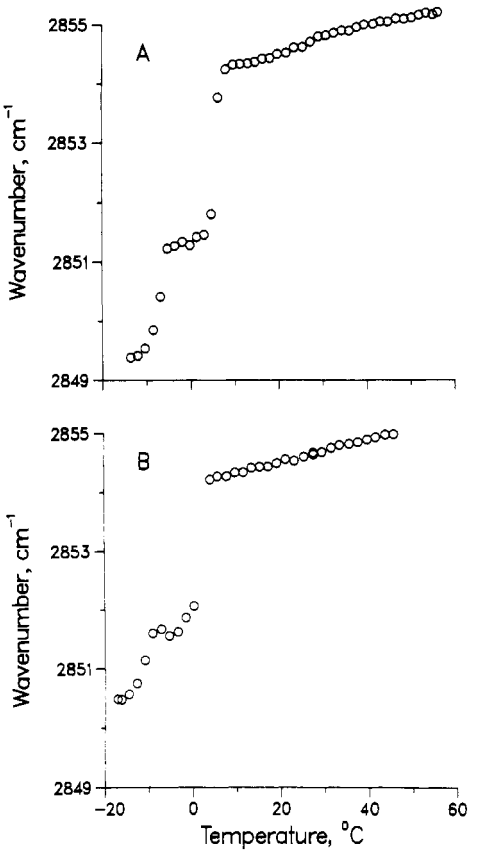

FIGURE 3: Temperature dependence of the wavenumber of the $\nu_s(CH_2)$ band in the infrared spectra of samples containing (A) 0.15 M DOPS–NH_4^+ and (B) 0.15 M LiCl and 0.15 M DOPS–NH_4^+ (DOPS/Li^+ molar ratio = 1.0). In both cases the samples were dispersed in D_2O buffer, pH 7.

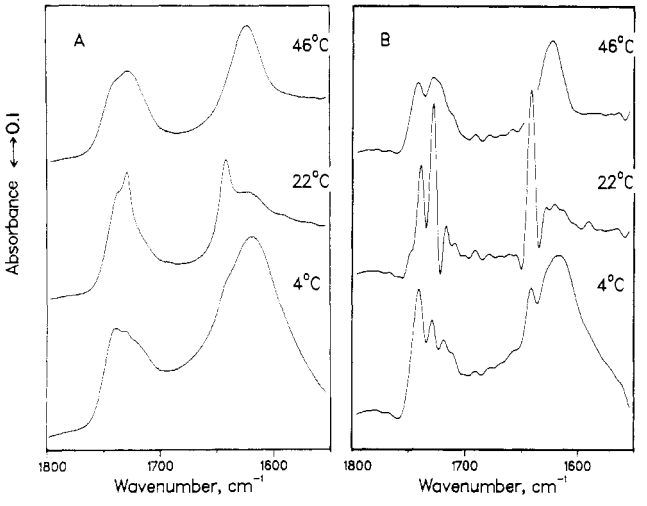

FIGURE 4: Infrared spectrum in the 1800–1550-cm^{-1} region of hydrated (D_2O buffer) POPS–NH_4^+ containing equimolar quantities of LiCl at 4, 22, and 46 °C. The traces in (B) are the result of deconvolution (see Materials and Methods).

The molecular level events associated with the formation of the PS–Li^+ complexes are best studied by examination of the spectral features originating from vibrational modes of the head group. In the presence of Li^+, the spectra of POPS are markedly different from those of POPS–NH_4^+. Figure 4 shows the 1800–1550-cm^{-1} region of the spectra of POPS–Li^+ complexes (POPS/Li^+ molar ratio = 1.0) at temperatures corresponding to the three different states of the sample, i.e., below T_1, between T_1 and T_2, and above T_2. At temperatures below T_1, the gel phase of POPS–NH_4^+ coexists with the gel phase of POPS–Li^+. Between T_1 and T_2, the gel phase of POPS–Li^+ coexists with the liquid-crystalline phase of POPS–NH_4^+, and above T_2, both POPS–NH_4^+ and POPS–Li^+ are in the liquid-crystalline state. The spectral differences between POPS–NH_4^+ and POPS–Li^+ below T_1 become particularly evident when one compares the deconvolved spectra in Figures 1A and 4B. The three C=O stretching bands in the POPS–Li^+ spectrum, at 1740, 1726, and 1715 cm^{-1}, form a pattern similar to that observed in the spectrum of DMPS–Li^+ (Casal et al., 1987b). As the liquid-crystalline phase of POPS–NH_4^+ forms at 18 °C (see Figure 2B), the spectrum at 22 °C in Figure 4 reflects this phase change. The band at 1740 cm^{-1} decreases in intensity, and as a consequence the shoulder at 1745 cm^{-1} is now visible; at the same time the band at 1726 cm^{-1} increases in intensity. At 46 °C POPS–Li^+ is in the liquid-crystalline phase, and its spectrum shows two C=O stretching bands, at 1740 and 1720 cm^{-1}, similar to those in the spectrum of liquid-crystalline POPS–NH_4^+ (Figure 1A). The ester C=O stretching bands of the POPS–Li^+ complex are essentially the same as those obtained with DMPS–Li^+ (Casal et al., 1987b). Thus, the conclusions reached earlier concerning the DMPS–Li^+ complex (Casal et al., 1987b) are also applicable to POPS–Li^+. For instance, the conformational nonequivalence of the chain segments next to the ester C=O groups is also found in the POPS–Li^+ complex, and the wavenumbers of the C=O stretching bands are consistent with no "new" hydrogen bonds being introduced by Li^+ binding. The doubling of both C=O bands (1740 cm^{-1} from *sn*-1 and 1720 cm^{-1} from *sn*-2) of POPS–NH_4^+ upon addition of Li^+ (1745 and 1740 cm^{-1} from *sn*-1 and 1726 and 1715 cm^{-1} from *sn*-2) is consistent with Li^+ inducing a conformational change in the glycerol backbone. These conclusions are based on the arguments outlined earlier and are compatible with the currently accepted views regarding the carbonyl stretching modes in diacyl lipids (Levin, 1984, and references cited therein).

Table II: Molecular Areas at 30 mN/m of Natural and Synthetic Diacylphosphatidylserines Spread as Monolayers on 0.066 M Phosphate Buffer, pH 7.4, and the Parameter α ($=h_{1640}/h_{1620}$) Determined from the Infrared Spectra of the Same Compounds in Samples Containing Equimolar Amounts of Lipid and LiCl

diacylphosphatidylserine	area/molecule[a] (Å^2)	α^b
DMPS–NH_4^+	45.5	4.1[c] (50 °C)
ox brain PS–Na^+	62.0	2.5 (26 °C)
POPS–NH_4^+	63.7	2.7 (23 °C)
DOPS–Na^+	67.5	0 (−1 °C)

[a] Data from Demel et al. (1987). [b] In parentheses is given the temperature at which α was measured; these are about 10 °C above the gel to liquid-crystalline transition of each of the NH_4^+ or Na^+ salts of the lipids at pH 7. [c] From Casal et al. (1987b).

The carboxylate bands and especially the antisymmetric stretching mode, $\nu_{as}(CO_2)$, are particularly informative with regard to the interaction of POPS with Li^+. The deconvolved spectrum in Figure 4B shows that at 4 °C there are two bands for the $\nu_{as}(CO_2)$ mode, at 1621 and 1640 cm^{-1}. The band at 1621 cm^{-1} is due to the carboxylate group of uncomplexed POPS–NH_4^+, while the band at 1640 cm^{-1} is due to the carboxylate group in the POPS–Li^+ complex. The $\nu_{as}(CO_2)$ band at 1640 cm^{-1} indicates that Li^+ binds to the carboxylate group of POPS, replacing the water of hydration of this group and at the same time losing part of its own hydration shell. The same was found for DMPS–Li^+ (Casal et al., 1987b).

For comparison, it is useful to define a parameter α as the peak height ratio h_{1640}/h_{1620}. This empirical ratio is a measure of the extent of Li^+ binding since the "1640-cm^{-1}" band is typical of Li^+ complexes and the "1620-cm^{-1}" band is char-

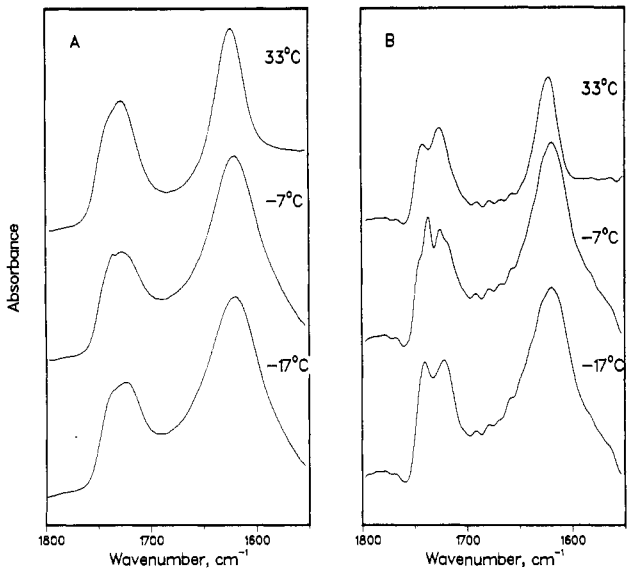

FIGURE 5: Infrared spectrum in the 1800–1550-cm^{-1} region of hydrated (D_2O buffer) DOPS–NH_4^+ containing equimolar amounts of LiCl at −17, −7, and 33 °C. The traces in (B) are the result of deconvolution (see Materials and Methods).

acteristic of uncomplexed fully hydrated PS. Table II lists the values of α (determined at T_1 + 10 °C, i.e., 10 °C above the gel to liquid-crystalline transition temperature of the corresponding NH_4^+ or Na^+ salts) derived from the spectra of DMPS–Li^+, POPS–Li^+, and DOPS–Li^+ at the same molar ratio lipid/Li^+ of 1.0. Also included in Table II are the areas per molecule as determined from monolayer measurements (Demel et al., 1987). The decrease in α with increasing area per molecule is a clear demonstration of the effect of the PS cross-sectional area on Li^+ binding.

Figure 5 shows the 1800–1550-cm^{-1} region of the infrared spectra of DOPS–NH_4^+ recorded at −17, −7, and 33 °C in samples containing equimolar amounts of LiCl and DOPS–NH_4^+. In all three spectra the $\nu_{as}(CO_2)$ mode gives only one band, at 1622 cm^{-1}, characteristic of a hydrated uncomplexed carboxylate group. There is no evidence of a band at 1640 cm^{-1}, characteristic of a dehydrated complexed carboxylate group, as observed in the spectra of DMPS–Li^+ and POPS–Li^+. The lack of a band at 1640 cm^{-1} in the spectra of DOPS–Li^+ leads to a value of zero for α (see Table II), indicating that in the case of DOPS there is no formation of a DOPS–Li^+ complex.

The ester carbonyl stretching bands of DOPS–Li^+ are also shown in Figure 5. At −17 °C the two C=O stretching bands are similar to those in the spectrum of DOPS–NH_4^+ below −11 °C, i.e., in the gel phase (not shown); similarly, at 33 °C the C=O stretching bands resemble those of DOPS–NH_4^+ in the liquid-crystalline phase. Thus, the presence of Li^+ has no effect on the ester carbonyl groups at temperatures below the gel to liquid-crystalline transition (T_1) and at temperatures above ice melting. In the temperature range between T_1 and ice melting, the ester carbonyl stretching bands are affected by the presence of Li^+ as exemplified in the spectrum recorded at −7 °C. The two ester carbonyl stretching bands are each split, giving rise to a total of four bands at 1745, 1737, 1726, and 1717 cm^{-1}. This pattern is characteristic of PS–Li^+ complexes; however, the bands in the DOPS–Li^+ spectrum are much broader than those of DMPS–Li^+ (Casal et al., 1987b) and POPS–Li^+ (Figure 4). This observation would be compatible with the formation of a DOPS–Li^+ complex only with DOPS in the liquid-crystalline phase and when the aqueous medium is frozen. In such a medium the activity of Li^+ at the lipid interface may be increased considerably due to Li^+ accumulation outside the ice lattice. Thus, the appearance of bands typical of PS–Li^+ complexes would indicate Li^+ binding as the result of a very high Li^+ activity.

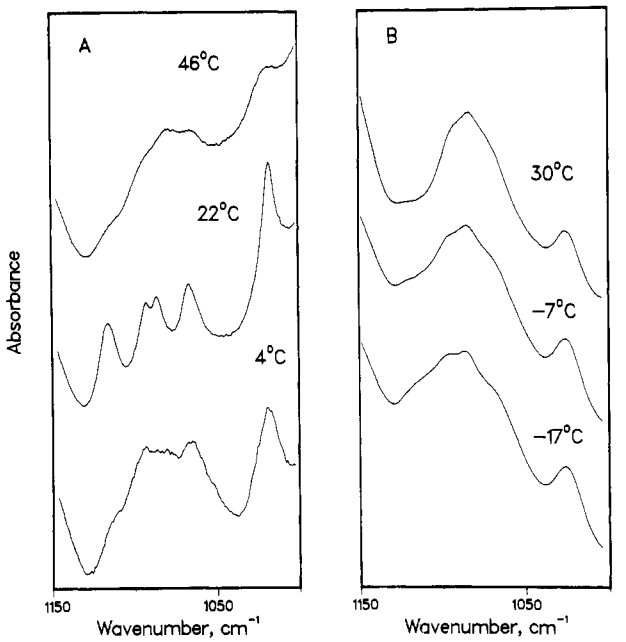

FIGURE 6: (A) Infrared spectrum in the 1150–1000-cm^{-1} region of hydrated (D_2O buffer) POPS–NH_4^+ containing equimolar amounts of LiCl at 4, 22, and 46 °C. (B) Infrared spectrum in the 1150–100-cm^{-1} region of hydrated (D_2O buffer) DOPS–NH_4^+ containing equimolar quantities of LiCl at −17, −7, and 30 °C.

The regions of the $\nu_s(PO_2)$ mode in the spectra of POPS–Li^+ and DOPS–Li^+ are shown in parts A and B of Figure 6, respectively. The spectrum of POPS–Li^+ at 4 °C is similar to that of POPS–NH_4^+ at 3 °C (Figure 1B); the same is true for the spectrum of POPS–Li^+ at 46 °C and that of POPS–NH_4^+ at 30 °C. However, the spectrum of POPS–Li^+ at 22 °C shows a pattern of bands typical of Li^+ complexes. This pattern is compatible with the phosphate group being in the gauche–gauche conformation (Casal et al., 1987a). In contrast, the spectra of DOPS–Li^+ shown in Figure 6B are the same as those of DOPS–NH_4^+, indicating that DOPS does not form a complex with Li^+.

The antisymmetric PO_2^- stretching mode, $\nu_{as}(PO_2)$, is at 1240 cm^{-1} in the spectrum of POPS–Li^+ (not shown), indicating that the phosphate group has lost its water of hydration as a consequence of Li^+ binding. However, the same mode in the spectrum of DOPS–Li^+ (molar ratio 1.0) is at 1224 cm^{-1} at all temperatures, indicating that the phosphate group is hydrated. This is compatible with DOPS not forming a complex with Li^+ and consistent with the observations discussed above.

(C) Infrared Spectra of POPS–Ca^{2+} and DOPS–Ca^{2+}. In this section we present the spectra of POPS–Ca^{2+} and DOPS–Ca^{2+} complexes of molar ratio lipid/Ca^{2+} = 1.0. Under these conditions there is no evidence of uncomplexed ammonium salts of POPS and DOPS. Also, there are no temperature-induced order–disorder transitions below 100 °C (see Table I), and therefore, the $\nu_s(CH_2)$ wavenumber was constant over the temperature range studied (5–80 °C).

Figure 7 shows the 1800–1550-cm^{-1} region of the spectra of POPS–Ca^{2+} at 10 and 53 °C (top) and DOPS–Ca^{2+} at −10 and 47 °C (bottom). There are four bands at 1741, 1729, 1719, and 1709 cm^{-1} in the POPS–Ca^{2+} spectrum and at 1741, 1729, 1718, and 1702 cm^{-1} in the DOPS–ca^{2+} spectrum. Therefore, the conclusions derived from DMPS–Ca^{2+} studied

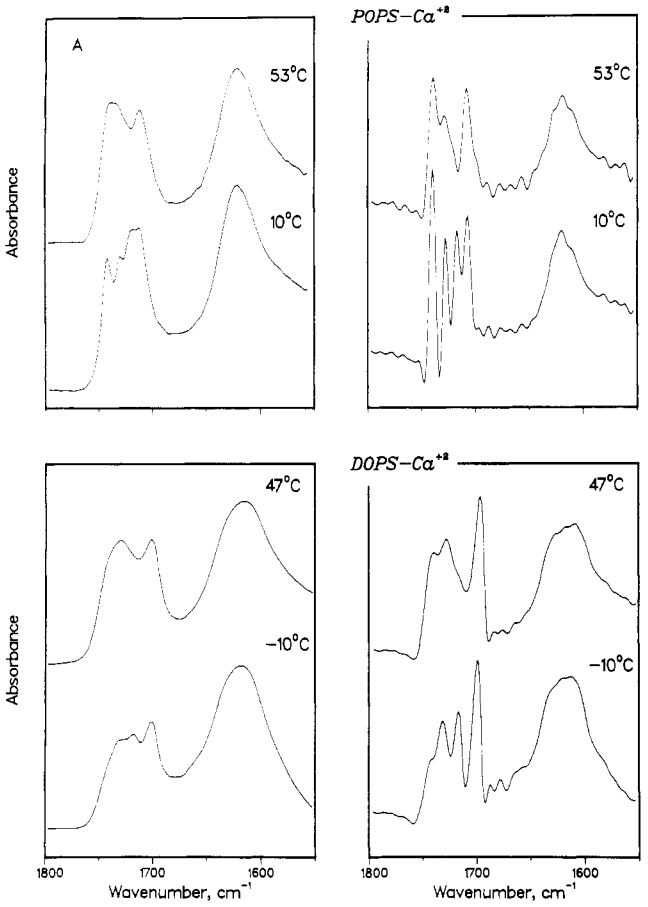

FIGURE 7: (Top) Infrared spectrum in the 1800–1550-cm^{-1} region of POPS–Ca^{2+} at 10 and 53 °C. (Bottom) Infrared spectrum in the 1800–1550-cm^{-1} region of DOPS–Ca^{2+} at −10 and 47 °C. The traces in the right-hand-side panels are the result of deconvolution (see Materials and Methods).

previously (Casal et al., 1987b) are also applicable to POPS–Ca^{2+} and DOPS–Ca^{2+}. In the spectra of PS–Ca^{2+} complexes the ester C=O bands are narrower than those in the spectra of PS salts with monovalent cations. This shows that the immobilization induced by Ca^{2+} is more pronounced than that induced by Li^+. There is a trend in the C=O ester bandwidths within the series DMPS–Ca^{2+}, POPS–Ca^{2+}, and DOPS–Ca^{2+}; the values of the bandwidths measured at 0.90 peak height are 4, 6, and 7.2 cm^{-1}, respectively. This indicates a decrease in Ca^{2+}-induced immobilization of PS with increasing molecular area or decreasing surface charge density. This trend is the same as that of the α values discussed for PS–Li^+ complexes (cf. Table II). The data of Figure 7 also show that the spectra of POPS–Ca^{2+} and DOPS–Ca^{2+} are temperature dependent; the band at 1719 cm^{-1} decreases in intensity with increasing temperature and eventually disappears in both cases. This process occurs over a relatively wide temperature range; the maximum rate of change is at 42 °C for POPS–Ca^{2+} and at 27 °C for DOPS–Ca^{2+}. No temperature-induced changes in the DMPS–Ca^{2+} carbonyl bands were found over the 5–80 °C temperature range (Casal et al., 1987b). The obvious reason for the disappearance of a carbonyl stretching band is motional interconversion of different chain rotational isomers (Bush et al., 1980); it reflects the larger mobility of the fatty acyl chains in the PS–Ca^{2+} complexes as the degree of unsaturation, and hence the molecular area, increases.

In the spectra of both POPS–Ca^{2+} and DOPS–Ca^{2+} there are bands indicative of hydrogen-bond formation involving the ester C=O groups: these are at 1709 and 1702 cm^{-1}, respectively. Similar findings were reported for ox brain PS–Ca^{2+} (Dluhy et al., 1983) and DMPS–Ca^{2+} (Casal et al., 1987b). These C=O bands do not show any temperature dependence.

The carboxylate groups remain hydrated in both POPS–Ca^{2+} and DOPS–Ca^{2+} as seen by the wavenumber of the $\nu_{as}(CO_2)$ mode (Figure 7); the $\nu_{as}(CO_2)$ bands are at 1622 and 1626 cm^{-1} in the spectra of POPS–Ca^{2+} and DOPS–Ca^{2+}, respectively, and are temperature independent. Thus, Ca^{2+} does not bind to the carboxylate group.

The Ca^{2+} complexes of POPS and DOPS are identical with the DMPS–Ca^{2+} complex with respect to the phosphate group. With all three PS the antisymmetric phosphate stretching band is at 1240 cm^{-1}, indicating that the phosphate group has lost its water of hydration by interacting with Ca^{2+}. As a result of Ca^{2+} binding, the conformation of the phosphate group becomes antiplanar–antiplanar as evident from the pattern of bands in the 1150–1000-cm^{-1} region.

CONCLUSIONS

The data presented here on Li^+ and Ca^{2+} complexes of POPS and DOPS, taken together with our previous study of DMPS (Casal et al., 1987b), give insight into the effects of metal ions at the molecular and submolecular level. The mode of Li^+ binding to PS is significantly different from that of Ca^{2+}. In the PS–Ca^{2+} complexes there are no order–disorder transitions below 100 °C. The phosphate group of PS chelates Ca^{2+}, and as a result this group loses its water of hydration and its conformation changes from gauche–gauche to antiplanar–antiplanar. The serine carboxylate group does not bind Ca^{2+}, but in the PS–Ca^{2+} complexes there appears new hydrogen bonding to one of the ester carbonyl groups. Examination of molecular models shows that when the phosphate group of PS adopts the antiplanar–antiplanar conformation, the head group lies approximately perpendicular to the bilayer plane. In such an arrangement the carboxylate group is farthest away from the lipid–water interface and the C=O group in the *sn*-2 chain is pushed toward the lipid–water interface. These features are compatible with the present infrared results that show the carboxylate group to remain hydrated and "new" hydrogen bonds to be formed involving the ester C=O groups.

Infrared experiments with the substituent molecule *sn*-glycero-3-phospho-L-serine (GPS) shed light on the role the PS bilayer plays in metal-ion binding. In contrast to PS bilayers, Ca^{2+} does not produce any changes in the spectra of GPS. Thus, it appears that tight binding of Ca^{2+} requires either a charged interface (surface) or chelation by appropriately spaced ligands. With increasing cross-sectional area of PS (and hence decreasing surface charge density), there is a change in the physical properties of the PS–Ca^{2+} complexes. There is a larger change in properties going from DMPS to POPS than from POPS to DOPS, which qualitatively correlates well with the increase in the respective molecular areas (see Table II).

In the case of PS–Li^+ complexes the effect of increasing the cross-sectional area (lowering the surface charge density) of the PS molecule is more dramatic than in the Ca^{2+} series. DMPS and POPS readily form crystalline complexes with Li^+, while DOPS does not . Also, the infrared spectra reveal that the affinity of DMPS for Li^+ is higher than that of POPS. In the PS–Li^+ complexes both the phosphate and serine carboxylate groups lose their water of hydration due to binding of Li^+; however, there are no hydrogen bonds formed to the ester C=O groups upon Li^+ binding. Contrary to the PS–Ca^{2+} complexes, in the Li^+ complexes the phosphate group

remains in the gauche–gauche conformation. It can be proposed that Li^+ bridges the carboxylate group of one PS molecule with the phosphate group of a neighboring molecule. Such a situation requires that both the carboxylate and phosphate groups lie in a plane approximately parallel to the bilayer plane. Further experiments to clarify this point are in progress.

In comparing the effects of Li^+ and Ca^{2+} on PS, we note that monolayer studies (Demel et al., 1987) have shown that Li^+ has little effect on the force–area curves of different phosphatidylserines; 100 mM Li^+ decreases the area per molecule by approximately 1 $Å^2$ at 30 mN/m. On the other hand, 10 mM Ca^{2+} induces decreases in area per molecule of 5–6 $Å^2$ at 30 mN/m (Demel et al., 1987). These results of the monolayer study are consistent with the present infrared data.

REFERENCES

Bush, S. F., Levin, H., & Levin, I. W. (1980) *Chem. Phys. Lipids 27*, 101–111.
Casal, H. L., & Mantsch, H. H. (1984) *Biochim. Biophys. Acta 779*, 381–401.
Casal, H. L., Mantsch, H. H., Paltauf, F., & Hauser, H. (1987a) *Biochim. Biophys. Acta 919*, 275–286.
Casal, H. L., Mantsch, H. H., & Hauser, H. (1987b) *Biochemistry 26*, 4408–4416.
Demel, R. A., Paltauf, F., & Hauser, H. (1987) *Biochemistry* (in press).
Dluhy, R. A., Cameron, D. G., Mantsch, H. H., & Mendelsohn, R. (1983) *Biochemistry 22*, 6318–6325.
Hauser, H., & Shipley, G. G. (1984) *Biochemistry 23*, 34–41.
Hauser, H., & Shipley, G. G. (1985) *Biochim. Biophys. Acta 813*, 343–346.
Hermetter, A., Paltauf, F., & Hauser, H. (1982) *Chem. Phys. Lipids 30*, 35–45.
Holwerda, D. L., Ellis, P. D., & Wuthier, R. E. (1981) *Biochemistry 20*, 418–428.
Jacobson, K., & Papahadjopoulos, D. (1975) *Biochemistry 14*, 152–161.
Kauppinen, J. K., Moffatt, D. J., Mantsch, H. H., & Cameron, D. G. (1981) *Appl. Spectrosc. 35*, 271–276.
Kurland, R. J., Hammoudah, M., Nir, S., & Papahadjopoulos, D. (1979) *Biochem. Biophys. Res. Commun. 88*, 927–932.
Levin, I. W. (1984) *Adv. Infrared Raman Spectrosc. 11*, 1–48.
Mantsch, H. H., Casal, H. L., & Jones, R. N. (1986) *Adv. Spectrosc. 13*, 1–46.
Mushayakarara, E., & Levin, I. W. (1982) *J. Phys. Chem. 86*, 2324–2327.
Ohki, S. (1982) *Biochim. Biophys. Acta 683*, 1–11.
Papahadjopoulos, D. (1978) *Cell Surf. Rev. 5*, 765–790.
Schou, M. (1976) *Annu. Rev. Pharmacol. Toxicol. 16*, 231–242.
Wilschut, J., Duzgunes, N., & Papahadjopoulos, D. (1981) *Biochemistry 20*, 3126–3133.

Further Consideration of Flavin Coenzyme Biochemistry Afforded by Geometry-Optimized Molecular Orbital Calculations

L. H. Hall,*,‡ M. L. Bowers,§,‖ and C. N. Durfor§,⊥

Department of Chemistry, Eastern Nazarene College, Quincy, Massachusetts 02170, and GTE Laboratories, Incorporated, Waltham, Massachusetts 02254

Received January 7, 1987; Revised Manuscript Received June 16, 1987

ABSTRACT: Investigation of lumiflavin and several other isoalloxazine ring derivatives has been carried out by geometry-optimized molecular orbital calculations. The results have provided insight into the flexibility of the flavin cofactor in the reduced and oxidized states, the regions of the fused three-ring system that should play an important role in flavin electron transfers, and the structural and functional role of the xylene and heteroatomic portions of the flavin system. The significance of these results is reviewed in relation to the experimentally identified chemical and biochemical properties of the flavin nucleotide coenzymes.

Flavin nucleotides are important biological cofactors that perform both single- and double-electron transfers. The isoalloxazine ring's accessibility to three oxidation states allows flavin coenzymes to couple the chemistry of two electron redox cofactors or organic molecules with molecular oxygen or cofactors transferring single electrons. The mechanism of dihydroflavin reaction with molecular oxygen has been studied extensively [for a review see Bruice (1984a,b)]. The protein environments of most flavin oxidases or monooxygenases enhance this reaction rate, yielding efficient oxidative catalysts or, in a special case, bioluminescence [for a review see Massey et al. (1980)]. In a variety of other proteins, interactions between the cofactor and its environment suppress the reoxidation of dihydroflavin by oxygen, which permits these flavoproteins to function effectively in electron transfers between proteins or between organic and inorganic substrates (Fox et al., 1982) and/or proteins. In addition to modifying chemical reactivity, interactions in the flavin nucleotide binding site can also profoundly affect the coenzyme's redox potential (Mayhew et al., 1975) or its accessibility to specific redox states (Ludwig et al., 1985).

Detailed information about the interactions of flavins with proteins and solvent can provide insight into the apoprotein's role in altering the geometric and electronic structures of the

* Author to whom correspondence should be addressed.
‡ Eastern Nazarene College.
§ GTE Laboratories.
‖ Present address: Cambridge Research Laboratory, Cambridge, MA 02139.
⊥ Present address: IGEN, Inc., Rockville, MD 20850.

0006-2960/87/0426-7401$01.50/0